Efficient creation of cellular micropatterns with long-term stability and their geometric effects on cell behavior

Ning-Ping Huang,[a] Hai Yu, Yan-Yan Wang, and Jun-Cai Shi
State Key Laboratory of Bioelectronics, School of Biological Science and Medical Engineering, Southeast University, Nanjing 210096, People's Republic of China

Xi Mao
Laboratory of Developmental Genes and Human Diseases, Medical School of Southeast University, Nanjing 210009, People's Republic of China

(Received 28 May 2011; accepted 2 September 2011; published 4 October 2011)

Cellular micropatterning with bio-adhesive and nonadhesive areas has attracted increasing interest for the precise design of cell-to-surface attachment in cell biology studies, tissue engineering, cell-based biosensors, biological assays, and drug development and screening. In this paper we describe a simple and efficient method to create a two-dimensional stable cellular microenvironment, which is based on (1) forming a protein-resistant *oligo(ethylene glycol) methyl ether methacrylate* polymer layer on the substrates via surface-initiated atom transfer radical polymerization; (2) placing a defined photomask on the substrate and exposing the substrate to ultraviolet light; and (3) immersing the patterned surface in a fibronectin solution to form cell-adhesive protein patterns in a cell-resistant background. The resulting surfaces are tailored into cell-adhesive and cell-resistant regions. Three different types of cells (NIH-3T3, PC12, bone marrow-derived mesenchymal stem cells) are seeded on such patterned surfaces to form cellular patterns. The geometric effects on cell behavior are investigated. The long-term stability is tested by NIH-3T3 fibroblasts and mesenchymal stem cells and excellent retention of cellular patterns is observed. The strategy illustrated here offers an efficient way to create a stable, patterned cellular microenvironment, and could be employed in tissue engineering to study the effect of micropatterns on the proliferation and differentiation of cells, and in particular mesenchymal stem cells. © *2011 American Vacuum Society*.
[DOI: 10.1116/1.3644381]

I. INTRODUCTION

In recent years, many researchers have cast light on understanding the effects of microenvironment on cell activities and functions, such as cell attachment,[1,2] proliferation[3,4] and differentiation.[5–7] Patterned living cells have shown promise in advancing the understanding of cellular processes, cell behavior and function in terms of gene function, cell-cell signaling, and cellular response to changes in environment conditions.[8–11] These studies have been directed towards organization of living cells and subcellular entities in a spatially controlled way. The efficient fabrication of well-controlled, stable cellular micropatterns is important in the development of cell-based biosensors, tissue engineering, drug screening, and fundamental studies of cell biology.

At present, a common theme of defining spatially controlled bio-adhesive patterns involves cell attachment on a background that resists protein adsorption. Therefore, an essential requirement is to chemically modify certain areas of the surface to render them nonfouling. Among various nonfouling molecular systems, ethylene glycol-related chemistries [oligo- or poly(ethylene glycol) (OEG or PEG)] have been widely used and display excellent protein- and cell-resistant properties. Ethylene glycol-based self-assembled monolayers (SAMs)[12–17] can be easily prepared at sufficiently high surface densities and are able to prevent nonspecific protein adsorption and cell adhesion. More recently, ethylene glycol-containing polymer brush surfaces have been prepared by means of atom transfer radical polymerization (ATRP) on various substrates including gold, silicon, glass, metal oxide surfaces, and polymer surfaces.[18–21] The thickness of the polymer brush can be finely tuned by varying the initiator surface graft density and the polymerization conditions.[18] The resulting polymer surface modifications are significantly thicker than those of the SAMs; thus creating an increased density of nonfouling groups on the surface and showing an increased resistance to nonspecific protein adsorption.[21] Moreover, it has been reported that the determining factor for the stability of a nonfouling film is the strength of the interaction between the passivating molecule and the substrate.[22] Therefore, covalent binding of the ethylene glycol-based polymer to reactively functionalized substrates is preferred. For the fabrication of cellular patterns, which are required to be immersed in complex cell culture media for further applications, an excellent nonfouling, cell-resistant film in the background is a key aspect for longer term culture of single cell or multicellular arrays. In this study, we employed poly(oligo(ethylene glycol) methyl ether methacrylate) (POEGMEMA) brushes as nonfouling films.

There has been a wide range of micropatterning techniques reported for the patterning of PEG and other

[a]Author to whom correspondence should be addressed; electronic mail: nphuang@seu.edu.cn

polymers, involving photolithography,[20,23–25] soft lithography,[17,19,26–28] laser scanning lithography,[29] ink-jet printing,[30] capillary force lithography,[31] and chemical lithography (e.g., utilizing electron beams to reduce nitro groups into amino groups, which can subsequently be used for selective binding of functional entities).[32–35] However, some techniques have limitations. For example, the need for clean-room access or specialized equipment makes some techniques inconvenient for biologists. Photolithography is not well suited for introducing either specific chemical functionalities, or delicate ligands required for bio-specific adsorption onto surfaces because of the requirement to remove photoresist with organic solvents. Microcontact printing, as one of the soft lithography techniques, has been widely employed for surface micropatterning by using stamps fabricated from an elastomeric material for pattern transfer. This technique is widely used due to its simplicity and flexibility. However, a stamping step prevents the large scale production of micropatterns, and the migration of "ink" during and after printing from the patterned regions needs to be properly controlled.

Recent studies have reported the creation of adhesive/nonadhesive patterns by UV degradation of SAMs or polymers. For example, a patterned MPC polymer layer has been achieved through prior patterning of ATRP initiators by UV irradiation and subsequent ATRP yielded brush structures whose dimensions were defined by the pattern of adsorbed initiator molecules.[36] The patterning of carbohydrate-grafted polymers has been carried out through prior patterning of amine-terminated SAMs by UV irradiation, followed by initiator functionalization, ATRP, and sugar-trapping.[37] By exposure of a PLL-*g*-PEG polymer layer to UV light, a simple and rapid method for cell patterning on polymer-coated large glass plates has been established.[38] However, the physisorption of PLL-*g*-PEG to glass substrates may limit the long-term stability of cellular patterns.[22] More recently, Ahmad *et al.*[39] presented a work on protein patterning by UV degradation of POEGMA, there a complete film of POEGMA was first formed and then selectively degraded to yield protein-binding areas. However, the cell-related issues based on this system have not yet been studied.

In this paper, we present a simple and effective method for fabricating a two-dimensional stable cellular microenvironment (Fig. 1). The strategy is based on (1) forming a UV-degradable cell-resistant POEGMEMA layer on the substrate via surface-initiated atom transfer radical polymerization (SI-ATRP); (2) placing a defined photomask on the substrate and removing the cell-resistant layer with ultraviolet light; (3) immersing the patterned surface in a fibronectin solution. The resulting substrate contains two different

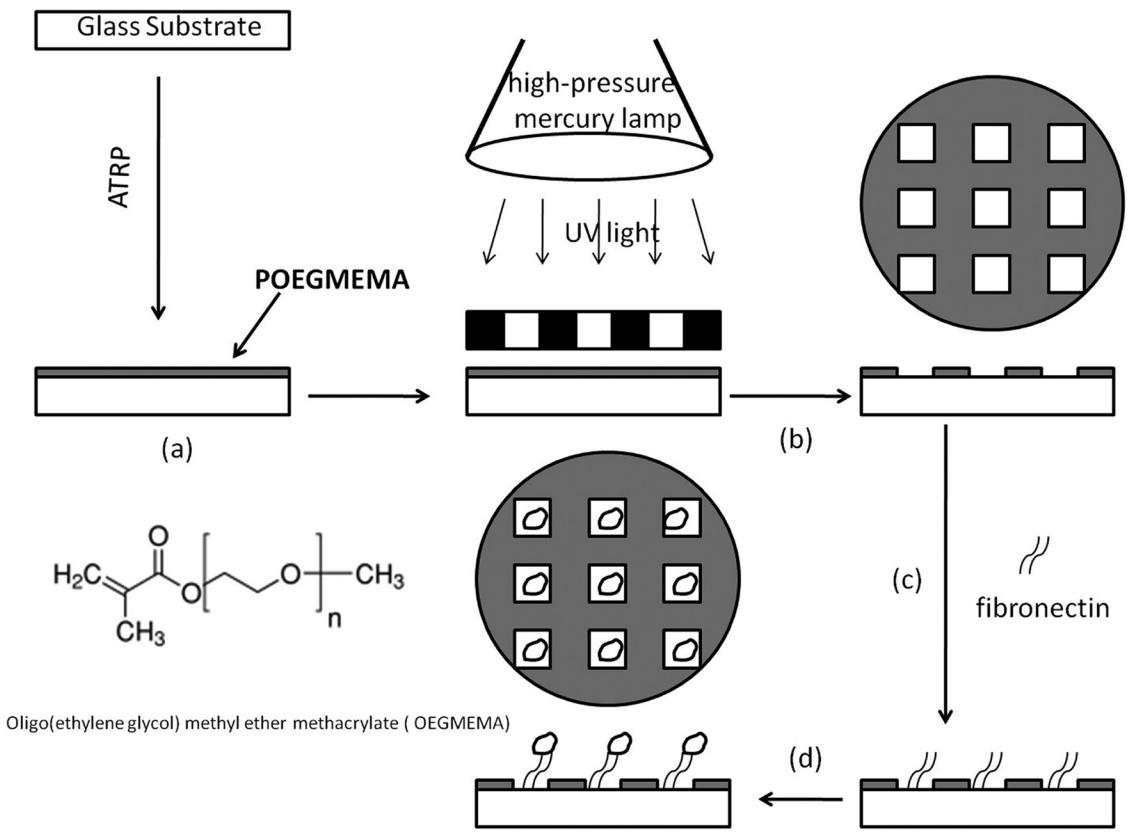

FIG. 1. Schematic formation of a cell-patterned surface via UV irradiation through a photomask. (a) POEGMEMA brushes were synthesized on glass substrates via SI-ATRP; (b) the polymer layers were irradiated by UV light from a high-pressure mercury lamp (quartz tube, 500 W) through a chromium mask on a quartz glass plate to create chemical patterns; (c) further exposed to a solution of 50 μg/mL fibronectin to form protein patterns; (d) after cell seeding, the cellular patterns were formed.

regions: cell-adhesive and cell-resistant regions. Three different types of cells (NIH-3T3 fibroblasts, neuronlike PC12 cells, bone marrow-derived mesenchymal stem cells) were seeded on patterned surfaces to form cellular patterns. The choice of the three cell types is based on: (1) 3T3 fibroblasts have been often used as model cells for testing the long-term stability of cellular patterns;[18,22,40] (2) patterning neuronal cells within a network formation array has potential applications in neurotoxicology and neurodevelopmental biology;[41–43] (3) stem cell-seeding density can strongly affect both differentiation and self-renewal, which has promise for wide applications in regeneration medicine and drug discovery fields.[7,11,25,28,44–46] In this paper, the long-term stability of cellular patterns and the influences of pattern area and distance of neighboring patterns on cell behavior such as cell morphology, migration, and proliferation are investigated.

II. MATERIALS AND METHODS

All chemicals were sourced from Sigma-Aldrich (USA) and used without further purification unless otherwise noted. Ultrapure water (18 MΩ cm^{-1}) obtained from an Easy Pure reverse osmosis system (Aquapro, Ever Young Enterprises Development Co. Ltd, China) was used both as a solvent and in cleaning processes.

A. SI-ATRP of OEGMEMA on glass slides

The process for oligo(ethylene glycol) methyl ether methacrylate (OEGMEMA) polymerization via SI-ATRP has been described elsewhere.[47] Briefly, glass slides were cleaned in piranha solution (H_2SO_4(98 wt %):H_2O_2(30 wt %) = 3:1(v:v)) at 80°C for 30 min, washed with copious ultrapure water, and dried in a nitrogen stream. Then the cleaned slides were immersed in aminopropyltriethoxysilane (10%) in ethanol for 30 min, rinsed with ethanol, and dried at 120°C for 3 h. Slides were then immersed in a solution of bromoisobutyryl bromide (1%) and triethylamine (1%) in dichloromethane for 30 min, rinsed with dichloromethane and ethanol, and dried under nitrogen. Next, Cu(I)Br (143 mg, 1.0 mmol), bipyridine (312 mg, 2.0 mmol) and OEGMEMA (M_n = 475, 8 g, 16.7 mmol) were added to a mixture of ultrapure water (degassed, 3 mL) and methanol (12 mL) with a stir bar. Glass slides were immersed in the degassed polymerization solution for 4 h at room temperature under nitrogen purge. Finally, the samples were rinsed with methanol and ultrapure water, and dried under nitrogen.

B. Preparation of chemical micropatterns via UV irradiation through a photomask

The chemical micropatterns were created by UV irradiation of the polymer samples in air using a high-pressure mercury lamp (quartz tube, 500 W, Beijing Lighting Research Institute, China) at 10 cm distance for a desired time period (30 min for POEGMEMA brushes) through a chromium mask on a 2-mm-thick quartz glass plate placed in contact with the polymer surface. The applied masks (Beijing Institute of Electronics, China) exhibit different UV-transparent squared patterns with the pattern area (region for cell adhesion) varying from 10 x 10 μm^2 to 90 x 90 μm^2 and the spacing distances between two neighboring patterns (cell-resistant region) from 50 μm to 250 μm. The pattern is shown in Fig. 1.

C. X-ray photoelectron spectroscopy analysis

X-ray photoelectron spectroscopy (XPS) analyses were performed at a takeoff angle of 90° (relative to the surface plane) using an ESCALAB 250 photoelectron spectrometer equipped with a concentric hemispherical analyzer in the standard configuration (Thermo Fisher Scientific, West Sussex, UK). The analyses were conducted at a chamber pressure of 10^{-9} mbar using a nonmonochromatic Al Kα source operating at 150 W. The instrument was run in the minimum-area mode using an aperture of 0.5 mm diameter. The analyzer was used in the fixed-analyzer transmission mode. Pass energies used for survey scans and detailed scans were 70 and 20 eV, respectively, the latter giving an experimental resolution of 1.0 eV for the Ag3d5/2 reference peak. All spectra were referenced to the aliphatic hydrocarbon C1s signal at 285.0 eV. Data were analyzed using a least-squares fit routine following Shirley background subtraction. Measured intensities (peak areas) were transformed into normalized intensities by taking into account their respective photoionization cross section corresponding to Wagner sensitivity factors.[48] Spectra were fitted with the XPSPEAK 4.1 software using the sum of an 80% Gaussian and 20% Lorentzian function.

D. Contact angle measurement

The water contact angles of POEGMEMA-modified surfaces before and after UV irradiation were measured by the sessile drop technique using a KSV CAM200 contact angle goniometer (KSV Instruments, Finland) under ambient laboratory conditions. A 4μL drop of distilled water was placed on the surface, and the contact angle was measured within 30 s. The measurements were performed at two different locations for each sample. The data from three independent samples were averaged and reported as mean ± standard error.

E. Optical waveguide lightmode spectroscopy

The waveguide chips coated with 6 nm SiO_2 (Microvacuum, Budapest, Hungary) were sonicated in 2-propanol for 10 min, extensively rinsed with ultrapure water, and dried in a nitrogen stream, followed by 2 min of oxygen-plasma cleaning in a Plasma Cleaner (13.56 MHz, Chengdu Mingheng Science & Technology, Chengdu, China). POEGMEMA brushes were generated on the cleaned waveguides by ATRP in the same way as mentioned in Sec. II A. UV irradiation of POEGMEMA-modified waveguides was performed as described in Sec. II B. without applying a mask.

Protein adsorption on the clean waveguides, POEGMEMA-modified waveguides, and POEGMEMA-modified waveguides after 30 min UV-irradiation was measured by Optical waveguide lightmode spectroscopy (OWLS). Samples were placed in the OWLS instrument (OW2400, Microvacuum, Budapest, Hungary) and equilibrated in a 10 mM HEPES ((4-(2-hydroxyethyl)piperazine-1-ethanesulfonic acid, *p*H 7.4) buffer. After reaching a flat baseline in ~30 min, 0.4 mL of goat Serum (Boster Biotechnology, Wuhan, China) was injected into the OWLS cuvette and incubated for 30 min at room temperature. The sample was then rinsed *in situ* with the HEPES buffer for ~30 min to remove the weakly adsorbed protein. Three experiments were repeated for each type of sample. Areal adsorbed mass density data were calculated from the adlayer thickness, and refractive index values were derived from the mode equations according to Feijter's formula.[49] A refractive index increment (dn/dc) value of 0.182 cm^3/g was used for the protein-adsorption calculations.[50]

F. Formation and visualization of protein patterns

Protein patterns were prepared by immersing the chemical-patterned substrates in a solution of 50 μg/mL fibronectin in 10 mM HEPES buffer solution for 30 min, subsequently rinsing with HEPES solution and blowing dry with nitrogen. To visualize the protein patterns, fibronectin was replaced by fluorescein isothiocyanate (FITC)-labeled fibrinogen (Beijing Biosynthesis Biotechnology Co., LTD) and the incubation took place in a dark room. The fluorescent samples were then imaged using an inverted fluorescence microscope (Nikon Ti, Japan).

G. Cell culture and imaging of cellular patterns

Before cell culturing, the chemical-patterned substrates were sterilized in 75% ethanol for 2 h, extensively rinsed with 10 mM HEPES solution and exposed to a solution of 50 μg/mL fibronectin in HEPES as described in Sec. II F. The above steps were carried out in a laminar-flow hood and all the solutions were sterilized through 0.22 μm filters.

To form cellular patterns, three different types of cells (NIH-3T3, PC12, bone marrow-derived mesenchymal stem cells) were employed. Fibroblasts (NIH-3T3, purchased from ATCC) and neuronlike cells (highly differentiated PC12, purchased from Shanghai Institute of Biochemistry and Cell Biology, SIBS, CAS) were maintained in Dulbecco's modified eagle medium(DMEM, Gibco, Canada) containing 10% fetal bovine serum (FBS, Gibco, Canada)and 1% penicillin/streptomycin antibiotics in a humidified incubator at 37°C with 5% CO_2. Bone marrow-derived mesenchymal stem cells (MSCs) were extracted from rat bone marrow as has been described previously.[51] MSCs were cultured in α-minimal essential medium (α-MEM, Sigma-Aldrich, USA) supplemented with 10% FBS and 1% penicillin/streptomycin antibiotics under standard culture conditions. When cells reached 80–90% confluence, they were trypsinized, counted with a hemocytometer, and seeded on the protein-patterned substrates placed in 24-well TCPS plates at a density of approximately 5000 cells/cm^2, then cultured in an incubator. The seeding density of PC12 cells was approximately 30 000 cells/cm^2. The medium was exchanged twice a week for the long-term measurements. Cell attachment to the patterned substrate was observed under a phase-contrast microscope. To clearly visualize the cellular patterns, the samples were washed with PBS and stained with 0.1 mg/mL acridine orange (Sigma-Aldrich) or with Alexa Fluor® 633 phalloidin at a dilution of 1:100 after fixation in darkness for 30 min, followed by rinsing with PBS to remove the residual dye and imaging through an inverted fluorescence microscope (Nikon Ti, Japan).

III. RESULTS AND DISCUSSION

A. Generation of POEGMEMA brushes on glass slides by SI-ATRP

Glass slides were cleaned with piranha solution, subsequently functionalized with amine-terminated organosilane and further modified with bromoisobutyryl bromide to present an ATRP initiator. Then the surface-tethered POEGMEMA brushes were synthesized via SI-ATRP. The POEGMEMA-coated surfaces were characterized by XPS, contact angle measurement, and OWLS.

Table I lists the intensities of the elements on different surfaces. Compared to the clean substrates, POEGMEMA-coated surfaces show a significant increase in the carbon intensity and a dramatic decrease in the silicon content. Only a small amount of the silicon signal was detected, suggesting the film thickness is close to the sample depth of XPS. The C1s high-resolution spectra of clean substrates and POEGMEMA-coated surfaces are shown in Fig. 2. Table II summarizes the experimental XPS binding energies (BEs) of the deconvoluted detailed C1s from the different surfaces together with the proposed assignments to chemical bonds/oxidation states based on observed chemical shifts. The C1s spectrum of clean glass surfaces [Fig. 2(a)] is dominated by a hydrocarbon peak (BE of 285.0 eV). Two smaller, additional peaks at higher binding energies are derived from oxygen-containing organic contaminants (C-O and OC=O). The C signal is due to unavoidable adventitious hydrocarbon

TABLE I. Normalized intensity of different elements on clean glass, POEGMEMA-coated surfaces, and various UV-irradiated POEGMEMA surfaces determined by XPS analysis.

	normalized intensities[a]			
surface	C	O	Si	N
Clean glass	12.3	66.3	21.4	
POEGMEMA	61.4	35.1	3.2	0.3
POEGMEMA-UV15min	17.5	62.0	19.1	1.4
POEGMEMA-UV30min	13.1	66.1	20.8	
POEGMEMA-UV45min	8.0	71.9	20.1	

[a]The measured peak areas divided by the corresponding sensitivity factors and normalized to 100% total intensity.

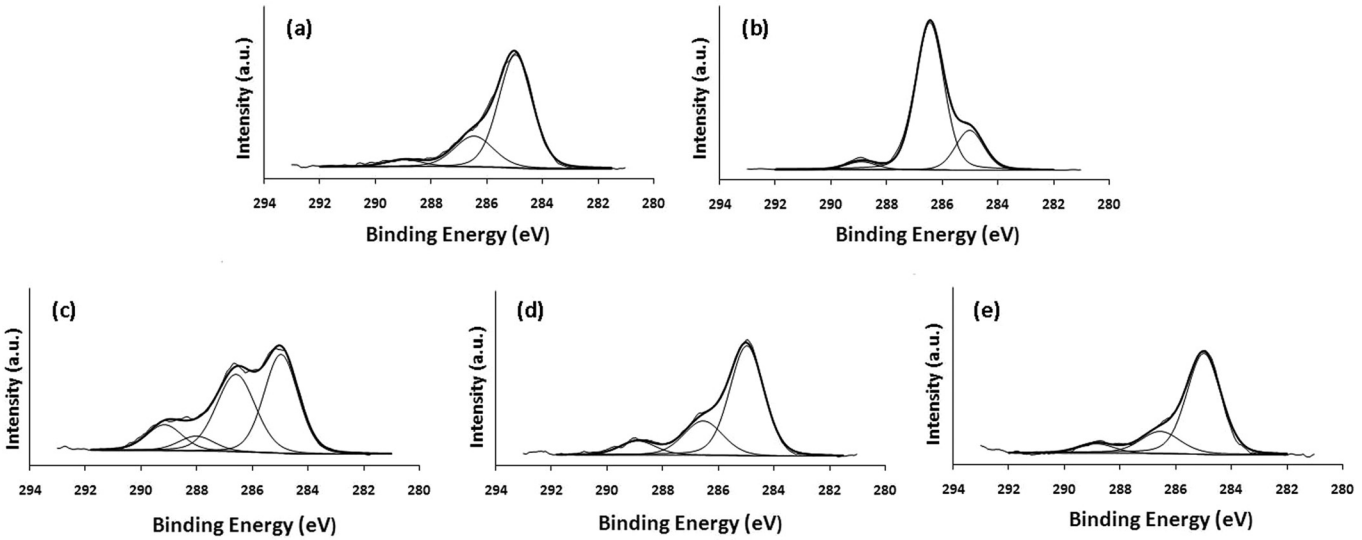

FIG. 2. High-resolution XPS spectra of the C1s region for the clean glass and POEGMEMA-coated glass: (a) clean glass, (b) POEGMEMA-coated surface, (c) POEGMEMA-coated surface after UV-irradiation for 15 min, (d) POEGMEMA-coated surface after UV-irradiation for 30 min, and (e) POEGMEMA-coated surface after UV-irradiation for 45 min.

contamination. The C1s spectrum of POEGMEMA-coated surfaces [Fig. 2(b)] is fitted with three peak components at BEs of 285.0, 286.5, and 289.0 eV, corresponding to the C-C/C-H, C-O, and O-C=O species, respectively (Table II). A significant increase in the C-O content was observed compared to the clean glass surface, due to the introduction of oligo(ethylene glycol) (OEG) groups at the surface. The spectral area ratio of two featured components on POEGMEMA surfaces (ether carbon: ester carbon) is 18:1, which is close to the theoretical ratio of 19:1 assuming that n=9 for the number of ethylene glycol repeats according to the molecular weight of OEGMEMA (see the molecular structure in Fig. 1).

Static water contact angle measurements further confirmed the presence of POEGMEMA brushes on the glass substrates after SI-ATRP. Piranha-solution cleaned glass slides were hydrophilic with a contact angle of ~10°, which increased to an average value of 39° after SI-ATRP of OEGMEMA (Table III), consistent with the values reported in literatures where contact angle of grafted polymer brushes with OEG side chains have been observed to be in the 35–46° range.[19,52,53]

OWLS experiments were performed to test the protein-resistant property of POEGMEMA-coated surfaces. The POEGMEMA-modified waveguide chip was prepared *ex situ* as described in Sec. II E and then assembled in the OWLS instrument. As plotted in Fig. 3, it was exposed to HEPES solution in order to obtain a stable baseline, then 100% serum was injected into the flow cell. After 30 min of adsorption, the serum solution was exchanged with 10 mM HEPES solution to remove the weakly adsorbed protein. For comparison, adsorption of serum on the unmodified SiO_2 waveguides was also tested. Figure 3 demonstrates that about 247 ± 20 ng/cm^2 of serum irreversibly adsorbed on the unmodified surface, while waveguide surfaces modified with POEGMEMA show a drastic reduction in protein adsorption. The amount of serum that remains adsorbed to the surface after serum adsorption and subsequent buffer rinsing is lower than the detection limit of the OWLS technique, that is, < 2 ng/cm^2. These results indicate the excellent nonfouling property of grafted POEGMEMA brushes.

TABLE II. XPS analysis (binding energy, relative peak area (%), assignment) of the C1s region for the clean glass, POEGMEMA-coated surfaces, and various UV-irradiated POEGMEMA surfaces.

surface	Peak1: 285.0 eV (%) C-C,C-H	Peak2: 286.5 eV (%) C-O	Peak3: 288.0 eV (%) C=O	Peak4: 289.0 eV (%) O-C=O
Clean glass	72.6	23.0		4.4
POEGMEMA	20.2	75.6		4.2
POEGMEMA-UV15min	43.3	38.6	6.6	11.5
POEGMEMA-UV30min	67.3	23.9		8.8
POEGMEMA-UV45min	74.6	18.1		7.3

TABLE III. Water contact angles of the clean glass, POEGMEMA-coated surface, and various UV-irradiated POEGMEMA surfaces.

surface	water contact angle(deg)
Clean glass	10 ± 1°
POEGMEMA	39 ± 1°
POEGMEMA-UV15min	38 ± 1°
POEGMEMA-UV30min	13 ± 1°
POEGMEMA-UV45min	10 ± 1°

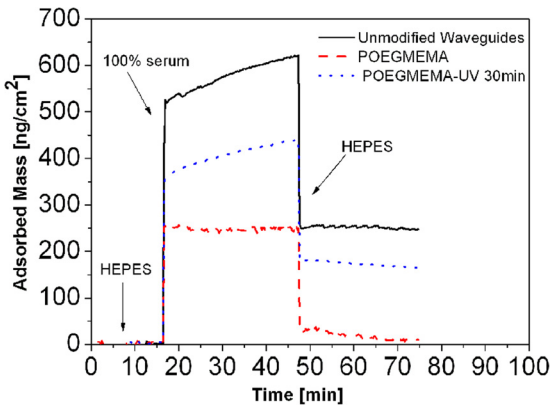

FIG. 3. (Color online) Real-time plots of serum adsorption measured by the OWLS technique on the unmodified waveguides, POEGMEMA-coated waveguides, and POEGMEMA-coated waveguides after 30 min UV-irradiation, followed by rinsing in buffer (10 mM HEPES, *p*H 7.4, T = 25°C).

B. UV- irradiated patterning of POEGMEMA surfaces

The two-dimensional micropatterned POEGMEMA surfaces were fabricated via UV-irradiation through a photomask contacting the glass slides coated with POEGMEMA brushes [Fig. 1(b)]. Various ultraviolet light sources have been used under ambient atmosphere or in a vacuum chamber for oxidation and etching of self-assembled monolayers or polymer surfaces.[36–39,54–57] UV light dissociates oxygen and generates activated oxygen species which have strong oxidative reactivity to organic molecules.[54] In this work, the UV irradiation was performed with a high-pressure Hg-lamp at 10 cm from the sample substrate under ambient atmosphere. For a 500 W high-pressure Hg lamp, it is estimated that the spectral intensity for wavelengths below 242 nm is ~70 mW/cm^2.[54]

After UV irradiation, POEGMEMA-coated surfaces show a significant increase in the silicon intensity (Table I), implying the degradation of POEGMEMA brushes. The change in surface chemistry resulting from the oxidation process during UV-irradiation was studied by detailed analysis of the C1s peak (Fig. 2). Figures 2(c), (d), and (e) show the C1s spectra of POEGMEMA-coated surfaces after UV irradiation for 15 min, 30 min, and 45 min, respectively. After UV-treatment for 15 min [Fig. 2(c)], the relative intensity of the C-O species from OEG groups decreased significantly, indicating the photodecomposition of OEG groups. Meanwhile, the C=O species at BE of 288.0 eV were newly formed and the intensity of the O-C=O species increased, which were likely due to the photooxidation reaction occurring in the main chain of the POEGMEMA unit with UV-generated active oxygen species. This process can generate new surface functional groups such as aldehyde and carboxylic acid or produce CO_2, which can lead to the shortening of the polymer chains.[55,56,58] When irradiation was extended up to 30–45 min [Figs. 2(d) and (e)], the intensity of the C-O species kept decreasing until OEG groups were completely decomposed. The C=O species (i.e., aldehyde groups) on the surface started to disappear because of a competition between generation of aldehydes and oxidization of aldehydes into carboxylic acid.[56] The resulting C 1 s spectra [Fig. 2(d) and (e)] were very similar to that from the cleaned glass surface [Fig. 2(a)]. Actually, the surface chemical composition of the 30-min UV-irradiated sample was very close to that of the cleaned glass substrate, i.e., background level (Table I). At this point, the sample surface is considered nearly identical to a bare glass after the organic coating has been largely decomposed and eliminated. This is also supported by water-contact angle data. When irradiation was extended up to 30–45 min, the contact angle of the sample finally decreased to ~ 10° (Table III), which is the same as that for the cleaned glass substrate. Based on the XPS and contact angle data, UV irradiation for 30 min or 45 min exhibited a similar decomposing effect on the POEGMEMA-coated surfaces. UV irradiation time of 30 min was then used for preparing protein and cellular patterns.

The protein adsorption on UV-irradiated POEGMEMA surfaces was monitored by OWLS. 170 ± 15 ng/cm^2 of serum irreversibly adsorbed on the UV-treated surface (Fig. 3), indicating protein adsorption at a level that should result in prominent cell adhesion and further cell growth to such UV-treated surfaces.

Based on above results, it appears that by applying a high-pressure Hg-lamp to irradiate nonfouling POEGMEMA surfaces through a photomask, chemical micropatterns with defined cell-adhesive and cell-resistant regions can be created.

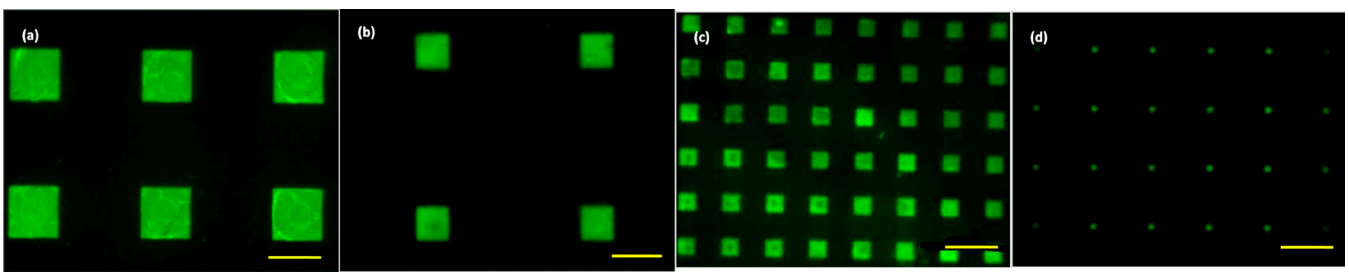

FIG. 4. (Color online) Fluorescence images of FITC-labeled fibrinogen micropatterns on POEGMEMA-coated glass slides previously UV-irradiated for 30 min through a photomask containing different squared pattern areas and spacing distances between two neighboring patterns: (a) pattern area 90 x 90 μm^2, spacing distance 150 μm; (b) pattern area 60 x 60 μm^2, spacing distance 250 μm; (c) pattern area 30 x30 μm^2, space distancing 50 μm; (d) pattern area 10 x10 μm^2, spacing distance 100 μm. Scale bars: 100 μm.

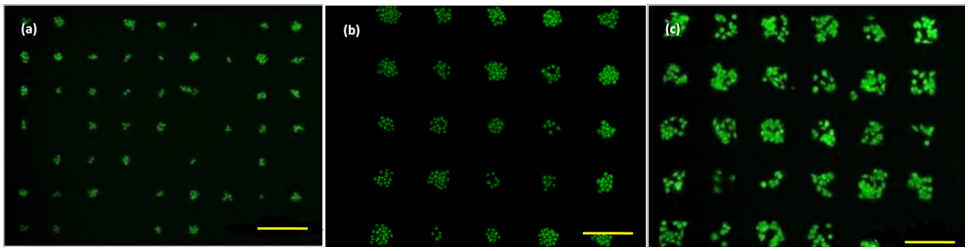

FIG. 5. (Color online) Fluorescence images of PC12 cells on fibronectin-patterned surfaces stained with acridine orange after 12 h of culture. (a) pattern area 30 x 30 μm^2, spacing distance 100 μm; (b) pattern area 60 x 60 μm^2, spacing distance 150 μm; (c) pattern area 90 x 90 μm^2, spacing distance 100 μm. Scale bars: 200 μm.

C. Formation of protein patterns

Protein patterns were spontaneously formed by incubating the chemically patterned substrates with fibronectin or FITC-labeled fibrinogen solutions; protein molecules exclusively adsorbed on the UV-irradiated regions (Fig. 1(c), Fig. 4). The square green arrays represent the protein-adsorbed, and thus, cell-adhesive region, corresponding to the UV-treated region of the POEGMEMA layer. It is clear that FITC-labeled protein could be hardly observed on the areas coated with POEGMEMA brushes. Furthermore, the green patterns are of regular square shape with distinct edges and correct size, implying that neglectable scattering of light or diffusion of ozone occurred into the masked regions and thus only the exposed POEGMEMA was degraded during the UV-patterning process. These results suggest that the protein resistance of the POEGMEMA coating is retained throughout the patterning process, and that the resulting patterns are of excellent quality for producing cellular patterns.

D. Cellular micropatterns and their geometric effects on cell behavior

Based on above obtained fibronectin-patterned POEGMEMA surfaces, different types of cells were seeded and cultured under standard conditions. As an extracellular matrix protein, fibronectin can bind to transmembrane receptor proteins called integrins, thus promoting cell adhesion.[59] The cellular patterns could be preliminarily formed and observed within 3 h after cell seeding.

Figure 5 shows PC12 cells grown on the fibronectin-patterned POEGMEMA surfaces containing different pattern areas and spacing distances. After 12 h of culture, the cellular patterns were already clearly observed (Fig. 5). The PC12 cells were found to attach exclusively to the fibronectin patterns and not to the POEGMEMA background. The sizes and spacing distances of the resulting cellular patterns are in reasonable agreement with the designed pattern geometries. After a longer time of culture, different cell responses were apparent on different pattern structures (See supplementary material in Ref. 60 for PC12 cell responses to different pattern structures, Figure S1). There is a close correlation between the incubation time and the size of the nonadhesive regions that the cell can overgrow. If the application of the pattern is to observe cell-cell communication or the proliferation and migration of patterned cells,[61] a smaller spacing between pattern (adhesive) regions should be applied. While for the studies requiring well-controlled, stable cellular patterns for a number of investigations that range from cell adhesion and apoptosis to cell differentiation and phenotype expression, a larger spacing between adhesive regions is preferred.

Mesenchymal stem cells (MSCs) from bone marrow were also used to make cellular patterns. Earlier reports have demonstrated that stem cell-seeding density can affect both differentiation and self-renewal.[44,45] More recently, it has been found that cell shape has a strong influence on the differentiation of MSCs.[7,11,25,46] For the purposes of investigating and exploring such issues, surfaces with controlled cellular patterns provide attractive platforms. Figure 6 shows bone

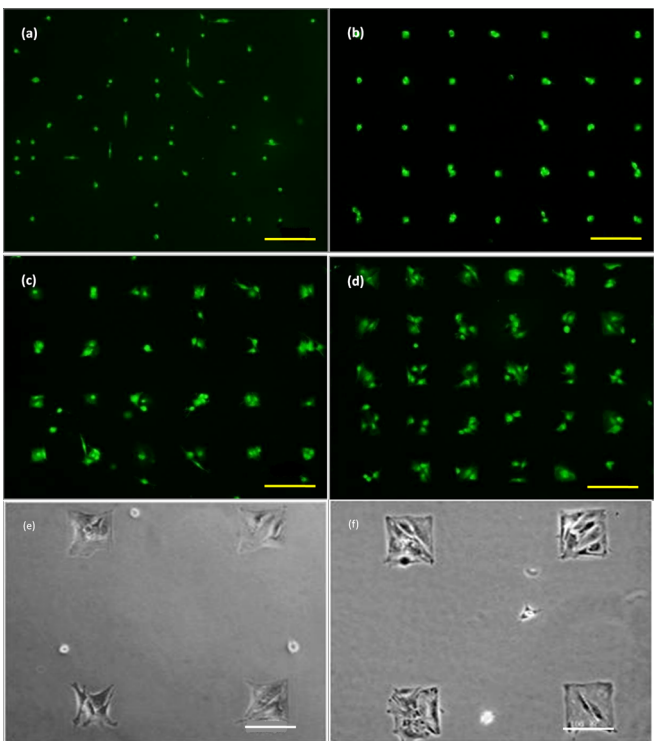

FIG. 6. (Color online) Bone marrow-derived mesenchymal stem cells (MSCs) at patterned surfaces. (a)–(d) Fluorescence image of MSCs on fibronectin-patterned surfaces stained with acridine orange after 36 h of culture. The squared pattern areas are (a) 10 × 10 μm^2, (b) 30 x 30 μm^2, (c) 60 x 60 μm^2, (d) 90 × 90 μm^2, respectively. (e) and (f) Phase-contrast images of MSCs on fibronectin-patterned surfaces (squared pattern area 90 × 90 μm^2, spacing distance 250 μm) after culture for (e) 1 day and (f) 3 days. Scale bars: 200 μm (a)–(d), 100 μm (e) and (f).

marrow-derived MSCs on patterned surfaces with different pattern areas. We can control the cell numbers in each square pattern elements; for example, only one cell was confined in the pattern element of $10 \times 10\,\mu m^2$ [Fig. 6(a)], providing an attractive testbed for carrying out single-cell research, and for the formation of neural networks.[42,43] Meanwhile, we designed pattern elements that are larger than the average cell size to allow multiple numbers of cells to stochastically load into each pattern; for example, in the pattern areas of $60 \times 60\,\mu m^2$ and $90 \times 90\,\mu m^2$ [Figs. 6(c) and (d)], providing each cell with a more uniform microenvironment than a non-patterned surface. Additionally, we were able to pattern small clusters of 1-5 MSCs, allowing them to experience cell-cell contact. Situations of cell-cell contact play an important role in maximizing self-renewal, that is, proliferation and maintenance of pluripotency, for mouse and human embryonic stem cells.[61–63] Stable multicellular aggregates (spheroids) also show a great potential for application in drug screening and discovery.[25,64]

Furthermore, the cells spread to different degrees depending on the size of the patterns and also display different cell shape. On the smaller pattern islands [Figs. 6(a) and (b)], the MSCs had little space to spread and retained a more spherical shape because they were restricted to a small area. In contrast, the MSCs on the larger pattern islands [Figs. 6(d) and (e)] were well-spread and flattened. Particularly, after three days of culture, the MSCs proliferated and spread extensively within the $90 \times 90\,\mu m^2$ pattern area [Fig. 6(f)]. They filled the pattern surface to full confluence, but were constrained to the square adhesive region. Therefore, cell density and cell shape can be controlled by adjusting the pattern geometry, which provides a practical platform to investigate cell response to various parameters of the cellular microenvironment; for example, geometric cues for directing the differentiation of stem cells.

E. Long-term stability of cellular patterns

The long-term stability of cellular patterns was investigated by seeding NIH 3T3 fibroblasts or mesenchymal stem cells onto fibronectin patterns in the POEGMEMA background and culturing for three weeks. 3T3 fibroblasts have been often used as model cells for stability tests,[18,22,40] The growth of fibroblasts on the patterned surfaces was periodically observed under a light microscope. At the beginning of the experiments (Fig. 7, Day 1), cells were able to sense the patterns and were largely confined to the adhesive areas. After prolonged culture time, cell proliferation was constrained to the $90 \times 90\,\mu m^2$ adhesive patches. We observed excellent retention of cellular patterns for more than 20 days (Fig. 7). Because the long-term stability of mesenchymal stem cells in patterns is critical for studying stem cell differentiation and tissue regeneration, the growth of MSCs on the patterned surfaces was also periodically investigated (Fig. 8). After seven days of culture, the MSCs were observed to be perfectly confined to the squared pattern areas. After 11 days of culture, the cellular patterns remained very clear although a few cells slightly spread over the border of a pattern element. On the day 15, the MSC started to touch the cells in neighboring patterns through cellular lamellipodia or filopodia. However, most cellular pattern elements remained well separated. Till the day 19, although the cellular patterns somehow could still be distinguished, it was clear that the MSCs started to bridge across multiple islands. Therefore, the integrity of the cellular pattern for MSCs can be well conserved until the day 14. Although it is not as good as for fibroblasts, the long-term stability of cellular patterns for MSCs at least meets the time period required for the differentiation of MSCs into diverse specialized cell types, including osteoblast, neurons, and myoblasts.[6,46,65] Additionally, the MSC micropatterns on a wafer scale after 8 days of culture are shown in Fig. 8(e). So far, few studies have been found to successfully show the MSC micropatterns after long-term culture. Above results demonstrate the feasibility of using our strategy for producing well-controlled, stable cellular patterns on the wafer scale, which is particularly desirable for applications requiring longer term culture of cells such as in (stem) cell differentiation and re-differentiation studies.

The approach of combining the SI-ATRP technique with UV-irradiation through a photomask to obtain cellular patterns in the background of POEGMEMA brushes has a number of distinct advantages: (1) UV irradiation directly induces the degradation of POEGMEMA brushes, leaving no toxic residue; (2) the mask can be reused many times, without introducing any contamination onto the surface; (3) patterns can be created on the scale of whole wafer surfaces with high throughput and reproducibility; (4) this is a one-step process that can be carried out in an ambient environment without using photoresist or any clean-room facilities; (5) the required UV light sources and photomasks are commercially available at reasonable costs. The cellular patterns

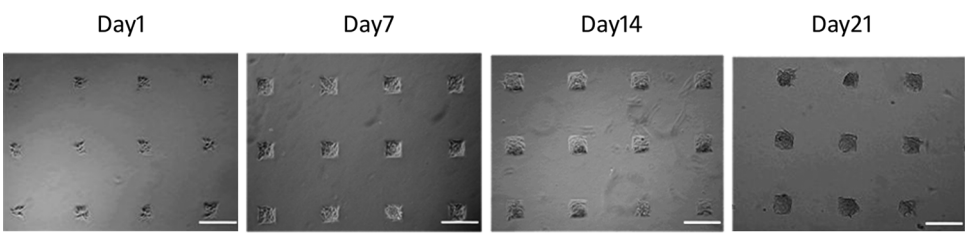

FIG. 7. Phase-contrast images of the long-term behavior of NIH 3T3 mouse fibroblasts on fibronectin patterns surrounded by POEGMEMA brushes. The patterns were squares of $90 \times 90\,\mu m^2$. The space between two neighboring patterns is 250 μm. Scale bars: 200 μm.

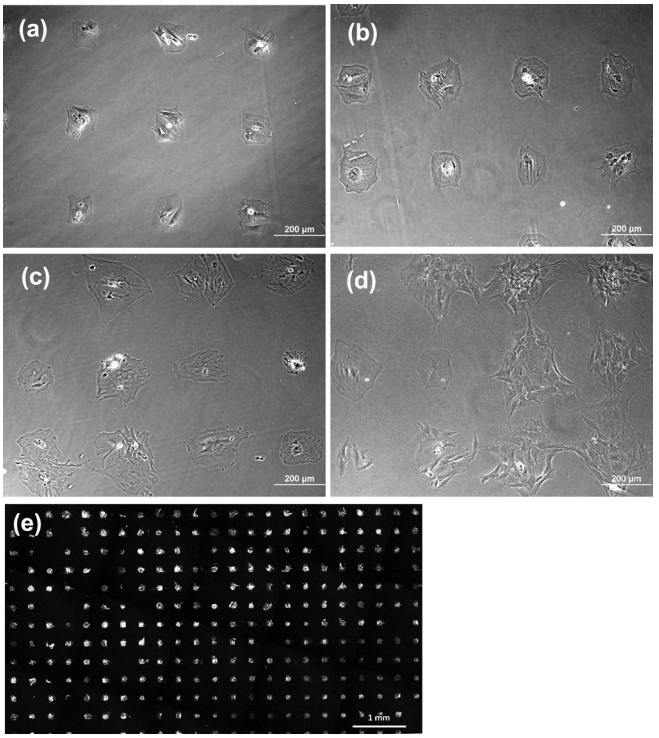

FIG. 8. Phase-contrast images of the long-term behavior of bone marrow-derived mesenchymal stem cells (MSCs) on fibronectin patterns surrounded by POEGMEMA brushes after culture for (a) 7 days, (b) 11 days, (c) 15 days, and (d) 19 days. (e) Fluorescence image of MSCs on fibronectin-patterned surfaces stained with Alexa 633 phalloidin after eight days of culture. All patterns were squares of 90 × 90 μm^2. The space between two neighboring patterns is 250 μm. Scale bars: 200 μm (a)–(d), 1 mm (e).

generated in this work are based on a background of POEGMEMA coatings on glass slides. Since the POEGMEMA brushes can be fabricated on a broad range of materials, including gold, silicon, and polymers,[20] the cellular patterns can be generated on various biomaterial surfaces using the technique described above; thus expanding the practical application in tissue engineering.

IV. CONCLUSIONS

We have developed an efficient and straightforward method to create chemically patterned surfaces for generating protein and cellular patterns combining SI-ATRP and UV-irradiation techniques. The patterns have been successfully prepared on the background of protein-resistant polymer coatings via UV irradiation through a photomask. This strategy provides a simple and cost-effective procedure for which clean-room conditions and photoresist are not required. The formation of cellular patterns from three different types of cells (PC12, NIH-3T3, MSCs) points to the versatility of this technique. This technique is also expected to be applied to generate cellular patterns within different nonfouling coatings on various material surfaces. Results of long-term stability demonstrate excellent retention of cellular patterns for more than 20 days culture time in the case of NIH 3T3 fibroblasts and for more than ten days in the case of mesenchymal stem cells, enabling studies requiring long-term stable cellular patterns, particularly those concerning the committed differentiation of stem cells. It is also evident that cell density and cell shape can be well controlled by adjusting the pattern geometry. Therefore, controlling chemical patterning would help significantly to develop purpose-specific cell-regulating cues in various biomedical applications including tissue engineering, cell-based biosensors, and basic cell biology studies.

ACKNOWLEDGMENTS

The authors would like to acknowledge Marcus Textor (Swiss Federal Institute of Technology, ETH Zürich, Switzerland) for his generous supply of waveguide chips and for constructive review of the manuscript. This work is supported by the National Science Foundation of China (Grant No. 30870626).

[1]C. S. Chen, M. Mrksich, S. Huang, G. M. Whitesides, and D. E. Ingber, Science **276**, 1425 (1997).
[2]L. Kam, W. Shain, J. N. Turner, and R. Bizios, Biomaterials **20**, 2343 (1999).
[3]M. M. Stevens and J. H. George, Science **310**, 1135 (2005).
[4]D. H. Kim, K. Han, K. Gupta, K. W. Kwon, K. Y. Suh, and A. Levchenko, Biomaterials **30**, 5433 (2009).
[5]M. J. Dalby, N. Gadegaard, R. Tare, A. Andar, M. O. Riehle, P. Herzyk, C. D. W. Wilkinson, and R. O. C. Oreffo, Nature Mater. **6**, 997 (2007).
[6]E. K. F. Yim, S. W. Pang, and K. W. Leong, Exp. Cell. Res. **313**, 1820 (2007).
[7]S. A. Ruiz and C. S. Chen, Stem Cells **26**, 2921 (2008).
[8]C. S. Chen, X. Y. Jiang, and G. M. Whitesides, MRS Bull. **30**, 194 (2005).
[9]J. Y. Lim and H. J. Donahue, Tissue. Eng. **13**, 1879 (2007).
[10]C. J. Bettinger, R. Langer, and J. T. Borenstein, Angew. Chem., Int. Ed. **48**, 5406 (2009).
[11]K. A. Kilian, B. Bugarija, B. T. Lahn, and M. Mrksich, PNAS **107**, 4872 (2010).
[12]P. Harder, M. Grunze, R. Dahint, G. M. Whitesides, and P. E. Laibinis, J. Phys. Chem. B **102**, 426 (1998).
[13]E. Ostuni, R. G. Chapman, M. N. Liang, G. Meluleni, G. Pier, D. E. Ingber, and G. M. Whitesides, Langmuir **17**, 6336 (2001).
[14]K. L. Prime and G. M. Whitesides, J. Am. Chem. Soc. **115**, 10714 (1993).
[15]M. Veiseh, B. T. Wickes, D. G. Castner, and M. Q. Zhang, Biomaterials **25**, 3315 (2004).
[16]N. P. Huang, R. Michel, J. Voros, M. Textor, R. Hofer, A. Rossi, D. L. Elbert, J. A. Hubbell, and N. D. Spencer, Langmuir **17**, 489 (2001).
[17]D. Falconnet, A. Koenig, T. Assi, and M. Textor, Adv. Funct. Mater. **14**, 749 (2004).
[18]H. W. Ma, J. H. Hyun, P. Stiller, and A. Chilkoti, Adv. Mater. **16**, 338 (2004).
[19]H. W. Ma, D. J. Li, X. Sheng, B. Zhao, and A. Chilkoti, Langmuir **22**, 3751 (2006).
[20]A. Hucknall, A. J. Simnick, R. T. Hill, A. Chilkoti, A. Garcia, M. S. Johannes, R. L. Clark, S. Zauscher, and B. D. Ratner, Biointerphases **4**, 50 (2009).
[21]J. Ladd, Z. Zhang, S. Chen, J. C. Hower, and S. Jiang, Biomacromolecules **9**, 1357 (2008).
[22]J. W. Lussi, D. Falconnet, J. A. Hubbell, M. Textor, and G. Csucs, Biomaterials **27**, 2534 (2006).
[23]J. M. Karp, Y. Yeo, W. L. Geng, C. Cannizarro, K. Yan, D. S. Kohane, G. Vunjak-Novakovic, R. S. Langer, and M. Radisic, Biomaterials **27**, 4755 (2006).
[24]H. Otsuka, A. Hirano, Y. Nagasaki, T. Okano, Y. Horiike, and K. Kataoka, ChemBioChem **5**, 850 (2004).
[25]W. J. Wang, K. Itaka, S. Ohba, N. Nishiyama, U. I. Chung, Y. Yamasaki, and K. Kataoka, Biomaterials **30**, 2705 (2009).
[26]R. S. Kane, S. Takayama, E. Ostuni, D. E. Ingber, and G. M. Whitesides, Biomaterials **20**, 2363 (1999).

[27]R. Michel, J. W. Lussi, G. Csucs, I. Reviakine, G. Danuser, B. Ketterer, J. A. Hubbell, M. Textor, and N. D. Spencer, Langmuir **18**, 3281 (2002).
[28]J. T. Connelly, J. E. Gautrot, B. Trappmann, D. W.-M. Tan, G. Donati, W. T. S. Huck, and F. M. Watt, Nat. Cell Biol. **12**, 711 (2010).
[29]M. S. Hahn, J. S. Miller, and J. L. West, Adv. Mater. **17**, 2939 (2005).
[30]A. Blau and T. Ugniwenko, Phys. Status Solidi B **4**, 1873 (2007).
[31]K. Y. Suh, Y. S. Kim, and H. H. Lee, Adv. Mater. **13**, 1386 (2001).
[32]U. Schmelmer, R. Jordan, W. Geyer, A. Gölzhäuser, and M. Grunze, Angew. Chem., Int. Ed. **42**, 559 (2003).
[33]A. Gölzhäuser, W. Eck, W. Geyer, V. Stadler, T. Weimann, and M. Grunze, Adv. Mater. **13**, 806 (2001).
[34]Q. He, Y. Tian, A. Küller, M. Grunze, A. Gölzhäuser, and J. Li, J. Nanosci. Nanotechnol. **6**, 1838 (2006).
[35]Q. He, A. Küller, M. Grunze, and J. Li, Langmuir **23**, 3981 (2007).
[36]R. Iwata, P. Suk-In, V. P. Hoven, A. Takahara, K. Akiyoshi, and Y. Iwasaki, Biomacromolecules **5**, 2308 (2004).
[37]R. Kamitani, K. Niikura, T. Onodera, N. Iwasaki, H. Shimaoka, and K. Ijiro, Bull. Chem. Soc. Jpn. **80**, 1808 (2007).
[38]A. Azioune, M. Storch, M. Bornens, M. Théry, and M. Piel, Lab Chip **9**, 1640 (2009).
[39]S. A. Ahmad, A. Hucknall, A. Chilkoti, and G. J. Legge, Langmuir **26**, 9937 (2010).
[40]W. K. Cho, B. Kong, H. J. Park, J. Kim, W. Chegal, J. S. Choi, and I. S. Choi, Biomaterials **31**, 9565 (2010).
[41]J. P. Frimat, J. Sisnaiske, S. Subbiah, H. Menne, P. Godoy, P. Lampen, M. Leist, J. Franzke, J. G. Hengstler, C. Van Thriel, and J. West, Lab Chip **10**, 701 (2010).
[42]S. Kelly, E. M. Regan, J. B. Uney, A. D. Dick, J. P. Mcgeehan, E. J. Mayer, F. Claeyssens, and B. B. Grp, Biomaterials **29**, 2573 (2008).
[43]F. Morin, N. Nishimura, L. Griscom, B. Lepioufle, H. Fujita, Y. Takamura, and E. Tamiya, Biosens. Bioelectron. **21**, 1093 (2006).
[44]K. A. Purpura, J. E. Aubin, and P. W. Zandstra, Stem Cells **22**, 39 (2003).
[45]E. H. Javazon, D. C. Colter, E. J. Schwarz, and D. J. Prockop, Stem Cells **19**, 219 (2001).
[46]R. Mcbeath, D. M. Pirone, C. M. Nelson, K. Bhadriraju, and C. S. Chen, Dev. Cell. **6**, 483 (2004).
[47]A. Hucknall, D. H. Kim, S. Rangarajan, R. T. Hill, W. M. Reichert, and A. Chilkoti, Adv. Mater. **21**, 1968 (2009).
[48]J. F. Moulder, W. F. Stickle, P. E. Sobol, and K. D. Bomben, *Handbook of X-ray Photoelectron Spectroscopy* (Perkin-Elmer Corp., Eden Prairie 1992).
[49]J. J. Ramsden, J. Stat. Phys. **73**, 853 (1993).
[50]J. J. Ramsden, D. J. Roush, D. S. Gill, R. Kurrat, and R. C. Willson, J. Am. Chem. Soc. **117**, 8511 (1995).
[51]X. Mao, C. L. Chu, Z. Mao, and J. J. Wang, Tissue Cell **37**, 349 (2005).
[52]L. Andruzzi, W. Senaratne, A. Hexemer, E. D. Sheets, B. Ilic, E. J. Kramer, B. Baird, and C. K. Ober, Langmuir **21**, 2495 (2005).
[53]W. H. Yu, E. T. Kang, K. G. Neoh, and S. P. Zhu, J. Phys. Chem. B **107**, 10198 (2003).
[54]K. L. Norrod, and K. L. Rowlen, J. Am. Chem. Soc. **120**, 2656 (1998).
[55]A. Hozumi, T. Masuda, K. Hayashi, H. Sugimura, O. Takai, and T. Kameyama, Langmuir **18**, 9022 (2002).
[56]S. Asakura, A. Hozumi, T. Yamaguchi, and A. Fuwa, Thin Solid Films **500**, 237 (2006).
[57]M. Montague, R. E. Ducker, K. S. L. Chong, R. J. Manning, F. J. M. Rutten, M. C. Davies, G. J. Leggett, Langmuir **23**, 7328 (2007).
[58]C.-Y. Xue and K.-L. Yang, J. Colloid Interface Sci. **344**, 48 (2010).
[59]T. A. Horbett. Colloids. Surf. B **2**, 225 (1994).
[60]See supplementary material at E-BJIOBN-6-301104 for PC12 cell responses to different pattern structures, Figure S1.
[61]A. Rosenthal, A. Macdonald, and J. Voldman, Biomaterials **28**, 3208 (2007).
[62]Q. L. Ying, J. Nichols, I. Chambers, and A. Smith, Cell **115**, 281 (2003).
[63]M. Amit, M. K. Carpenter, M. S. Inokuma, C. P. Chiu, C. P. Harris, M. A. Waknitz, J. Itskovitz-Eldor, and J. A. Thomson, Dev. Biol. **227**, 271 (2000).
[64]M. Håkanson, M. Textor, and M. Charnley, Integr. Biol-Uk **3**, 31 (2011).
[65]A. J. Engler, S. Sen, H. L. Sweeney, and D. E. Discher, Cell **126**, 677 (2006).